Maritime Research and Technology

MRT
ISSN 2812-5622

http://dx.doi.org/10.21622/MRT.2025.04.1.1110

Surge Behavior in Alexandria Western Harbor and its Correlation to Dominant Meteorological Condition

[1] Mohamed Mahmoud Mohamed Heiba,
[2] Tarek Mohamed El-Geziry,
and [3] Sameh Tawfik Abd Elfattah

[1] Arab Academy for Science, Technology and Maritime Transport (AASTMT).
[2] National Institute of Oceanography and Fisheries (NIOF).
[3] Marine Engineering Technology, Arab Academy for Science, Technology and Maritime Transport (AASTMT).

Emails: mohamed.Heiba@aast.edu, tarekelgeziry@yahoo.com, samehtawfik@aast.edu

Received on: 28 November 2024 Accepted on: 30 December 2024 Published on: 14 January 2025

ABSTRACT

Purpose: *This study examines the relationship between wind characteristics (speed and direction), atmospheric pressure, and surge heights at Alexandria Western Harbor (AWH) over 19 months (June 2018–January 2020).*

Approach/Design/Methodology: *Hourly Sea level data collected using a radar sensor at the harbor pier, and concurrent meteorological data from Ras-El Tin weather station were analyzed. Surge heights were extracted from observed sea level data using the MATLAB-based T-Tide package, incorporating astronomical tides and surges.*

Findings: *The results show that surge heights ranged from 29.2 cm to 68 cm, with a mean of 50.7 cm. The predominant wind directions were NW, WNW, and W, with speeds varying from 0 to 19.55 m/s (mean: 5.98 m/s). Atmospheric pressure ranged from 1001 to 1026.6 millibars, with a mean of 1011.81 millibars. Wind speed emerged as the primary driver of surge variation (correlation coefficient: 0.25), while atmospheric pressure exhibited an inverse correlation (-0.35).*

Key-words:
Alexandria Western Harbor, Surges, Wind regime, Atmospheric pressure, Correlation.

MRT
ISSN 2812-5622
http://dx.doi.org/10.21622/MRT.2025.04.1.1110

INTRODUCTION

This research provides a comprehensive analysis of surge behavior in Alexandria Western Harbor (AWH), emphasizing the influence of meteorological factors such as wind and atmospheric pressure over a 19-month period. Relationships between surge heights and meteorological parameters, including wind speed, wind direction, and atmospheric pressure, were examined using Microsoft Excel charts to determine trend line slopes, regression equations, and correlation factors for each month. Additionally, months from June to December 2019 were reanalyzed to identify similarities and differences between the same months in different years.

The impact of strong winds on coastal areas primarily depends on wind direction, speed, and the exposure of the coastline to prevailing winds. Meteorological patterns tend to follow a recurring annual cycle, with maximal surge threats arising from specific combinations of wind force and atmospheric pressure. Sea level fluctuations consist of two main components: the astronomical component, driven by gravitational forces causing tides, and the irregular component, influenced by variations in atmospheric pressure, wind, and waves (McInnes et al., 2015; Ozturk & Yuksel, 2023).

Sea level data are processed to predict tidal cycles and understand the hydrodynamics of the sea, including the influence of tidal forces (Paugh, 2004). Astronomical tidal parameters, such as amplitudes and phases, are governed by geographic location (Bryden et al., 2007; Maher Hendy, El-Geziry et al., 2021). The non-tidal component of sea level (surge) fluctuates at a lower frequency, reflecting seasonal coastal changes dominated by meteorological conditions (Ozturk & Yuksel, 2023).

Sea level rise (SLR) is a critical consequence of climate change, posing threats to low-elevation coastal regions worldwide, particularly in developing countries. Alexandria is identified as one of the region's most vulnerable to SLR, with projections of significant flooding by 2100 (Noby et al., 2022). Climate change contributes to SLR, leading to beach erosion, flooding, and ecosystem disruption (Ibrahim & El-Gindy, 2022; Nicholls & Cazenave, 2010). Since 1992, Alexandria coast has faced intensified SLR impacts, largely attributed to global warming and rising atmospheric temperatures (Noby et al., 2022b).

The IPCC AR5 (2013) reported a global mean sea level rise of 0.19 m between 1901 and 2010, with an acceleration to 0.32 cm/year from 1993 to 2010 (Stocker et al., 2013). Studies further indicate a global mean sea level rise rate of 0.1– 0.2 cm/year over the last century, with ongoing increases expected due to oceanic thermal expansion (Church & White, 2011; Hendy et al., 2021), while other studies state that a clear evidence of global mean sea level has raised at rate of 0.16 to 0.19 cm/year (Zerbini & Vincent Rocco, 2014). The Mediterranean Sea has exhibited rising sea levels due to atmospheric pressure changes and thermal expansion, with the IPCC (2022) highlighting its susceptibility to climate change.

The Mediterranean's mean sea level has been rising at a rate of 12–15 mm/year since 1960, with projections of accelerated increases due to CO_2 emissions (Ibrahim & El-Gindy, 2022). However, this rate varies across the basin due to topographical, climatic, and hydrodynamic differences, such as longshore currents and storm frequency (Ibrahim & El-Gindy, 2022; Solomon et al., 2007). From 1993 to 2011, the Mediterranean experienced a linear sea level rise of approximately 0.3 cm/year due to ocean mass expansion and the North Atlantic Oscillation in winter (Tsimplis et al., 2013; Ibrahim & El-Gindy).

Alexandria, particularly its Western Harbor, is highly vulnerable to SLR, with an annual rise ranging between 0.17 and 0.3 cm (Frihy, 1992; Shaker et al., 2011; Said et al., 2012; Maiyza & El-Geziry, 2012; Maher Hendy, El-Geziry et al., 2021). The harbor's tides are semi-diurnal (El-Geziry, 2013), with astronomical tide heights of 20–30 cm and surge heights reaching 1 m. Planning and adaptation are essential to mitigate the impacts of extreme sea levels, which are governed by local factors such as bathymetry, tidal characteristics, and wind patterns (Andrée et al., 2022).

Wind direction and speed are expected to change in the short term due to climate change, influencing surge behavior (Hdidouan & Staffel, 2017; Gumuscu et al., 2024). Weather patterns significantly impact surge variations, with studies showing that 75% of surge fluctuations in Graude-la-Dent, Rhône Delta, France, were linked to weather conditions (Saad et al., 2011). Onshore winds generally produce positive surges, while offshore winds result in negative surges. Winds parallel to the coast can generate both surge types due to Ekman transport (Weisberg & Zheng, 2006; Heidarzadeh et al., 2023).

Atmospheric pressure can influence sea level readings by 0.1 to 0.4 m (Couriel et al., 2014; Ozturk & Yuksel, 2023).

This research investigates the regression and correlation factors between wind direction, wind

MRT
ISSN 2812-5622
http://dx.doi.org/10.21622/MRT.2025.04.1.1110

speed, atmospheric pressure, and sea level variations in Alexandria Western Harbor. By analyzing hourly sea level data over 19 months, it explores meteorological influences on surge behavior and highlights the sea level responses to wind and atmospheric pressure changes across the harbor.

DATA AND METHODS OF ANALYSIS

The study area, located in Alexandria Western Harbor on the southern coast of the eastern Mediterranean's Levantine Basin, provides a sheltered setting for the sea level radar. This protected location ensures consistent and stable data readings, maintaining accuracy and reliability.

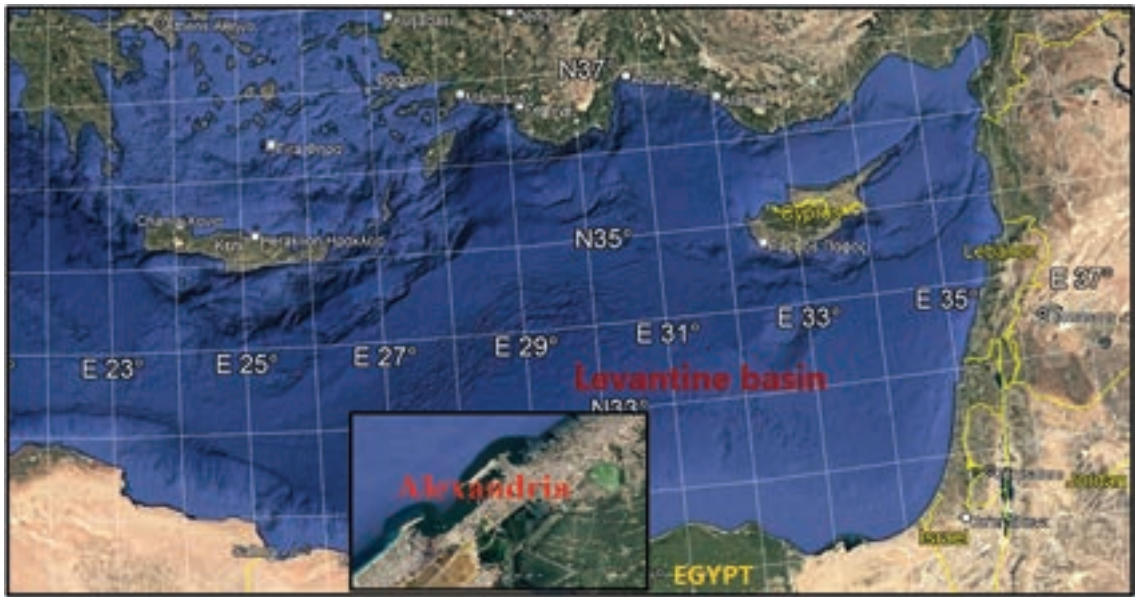

Fig. 1. Alexandria, Egypt coast in Levantine basin- Mediterranean Sea

The research employs quantitative analytical methodology, utilizing observed sea level heights referenced to the chart datum of Alexandria Western Harbor alongside meteorological parameters for wind and atmospheric pressure.

Sea level data were collected using a CS475A radar sensor installed in the interior of the harbor at coordinates (31°11′55.55″N, 029°52′22.10″E). The dataset is of high quality and reliability, with minimal gaps in observations. Any missing data, accounting for only a few hours during the entire period, were interpolated mathematically. Figure 2 illustrates the standard deviation graph for the observed sea level data collected in Alexandria Western Harbor.

The dataset comprises 13,986 hours of observations gathered over 582.75 days, spanning from June 5, 2018, to January 9, 2020. The data were processed using the T-Tide software, applying classical harmonic analysis through complex algebraic equations. This approach models tidal signals as the sum of fixed-frequency sinusoids, while residuals—primarily surge values—are statistically analyzed using a Gaussian curve with no time correlation (Pawlowicz et al., 2002).

Sea level variations consist of two primary components: tidal data and surges, each with distinct characteristics, frequencies, and energy levels. The Mediterranean Sea's rising sea level, driven by climate change, is influenced by atmospheric pressure changes and the steric effect (Gomis et al., 2008; Hendy et al., 2021).

Wind speed and direction data from the 19-month observation period were analyzed to create a wind rose diagram and visualize the dominant wind patterns at Alexandria Western Harbor. These data were processed using the OpenAir package in RGui software to develop programming codes. The relationship between wind speed, wind direction, atmospheric pressure, and surge heights was further analyzed using Microsoft Excel to calculate and graph trendlines, regression equations, and correlations.

Meteorological data, including wind direction, wind speed, and atmospheric pressure, for the study period (June 2018 to January 2020), were sourced from the meteorological station at Ras-El Tin, located at Alexandria Western Harbor.

MRT
ISSN 2812-5622
http://dx.doi.org/10.21622/MRT.2025.04.1.1110

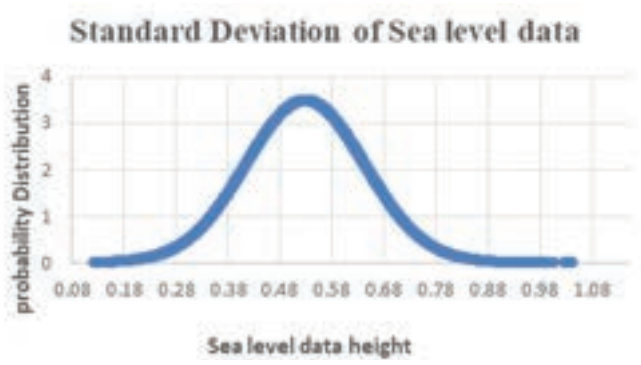

Fig. 2. Sea level data standard deviation

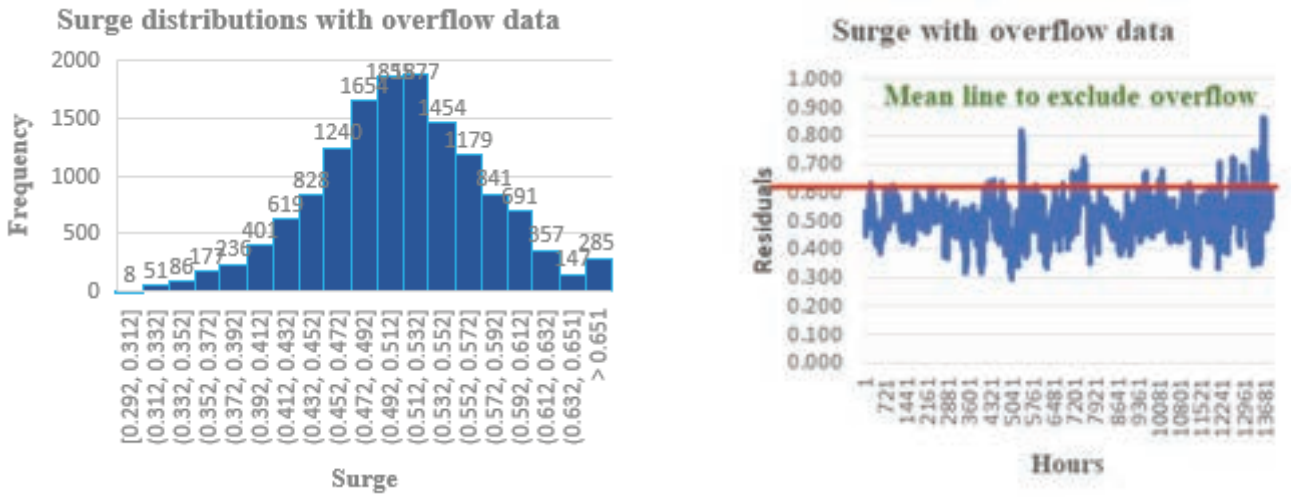

Fig. 3. Surge with overflow data: at the left, the Histogram represents Surge data distribution, at the right the graph represents Surge data with overflow data

Sea level variations consist of two primary components: tidal data and surge, each with distinct characteristics, frequencies, and energy levels. In the Mediterranean Sea, rising sea levels are driven by climate change and influenced by atmospheric pressure changes and the steric effect (Gomis et al., 2008; Hendy et al., 2021).

These relationships are captured in the following conservative equation, which links mean sea level, tidal, and surge components:

variances (mean sea level, tide, and surge);

$$X(t) = Z_0(t) + T(t) + S(t) \quad \text{..... (1) (Paugh et al., 2014)}$$

Where:

$X(t)$ Sea level at time series

$Z_0(t)$ mean sea level slowly changed with time

$T(t)$ tidal component of sea level data

$S(t)$ Residuals (Surge, Seiches, and possible measurements errors)

Average variance s^2 for Alexandria Sea level data (June 2018- January 2020) = 130.87 cm^2

Standard deviation for Sea level data = 11.4 cm

Non-tidal components were filtered to exclude overflow data and adjusted for a maximum surge of 68.4 cm to remove uncertain observations, which occurred only once during the study period. This adjustment is represented in Figure 3, where:

- The left panel shows a histogram of surge value distribution.
- The right panel illustrates surge data, including overflow values.

Surge data were examined for spikes and extremes in hourly observations across the entire period. These outliers were adjusted to align with a normal distribution curve (Gaussian curve), as shown in Figure 4. The average maximum surge height was determined to be 0.68 m. This process ensures the reliability of surge data and highlights the critical extremes during the observation period.

MRT
ISSN 2812-5622
http://dx.doi.org/10.21622/MRT.2025.04.1.1110

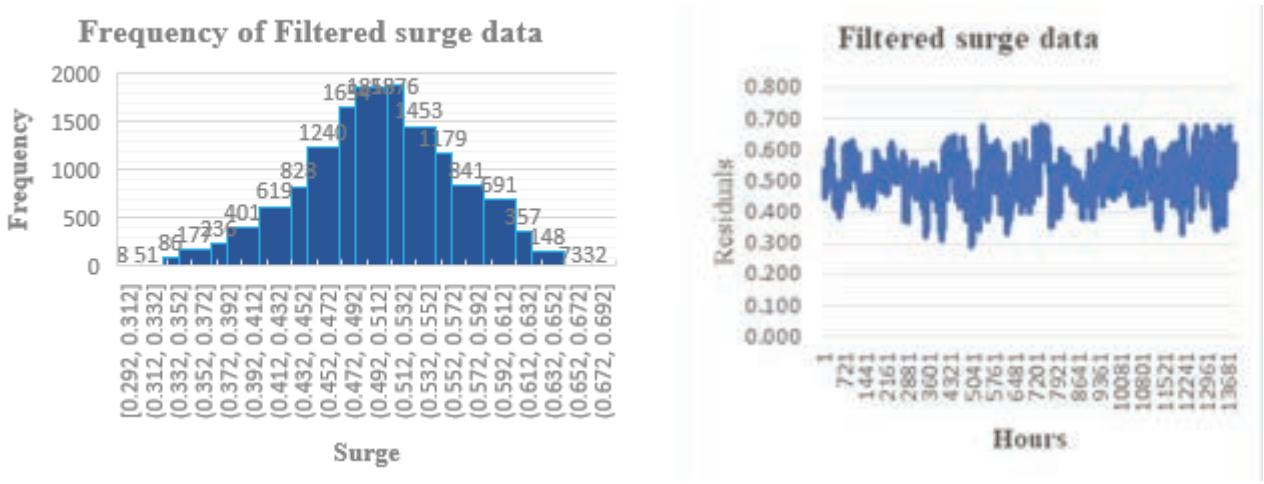

Fig. 4. Filtered Surge: at the left the Histogram represents Surge data distribution, at the right the Surge data graph without overflow data

The relationship between wind direction, wind speed, and atmospheric pressure with surge height was analyzed using a combination of RGui programming software and Microsoft Excel. Mean sea level data for the observation period (June 5, 2018, to January 9, 2020) were calculated and graphed using RGui. The mean tidal range was determined using the following equations:

$$\text{Mean High Water} = (1/N) \sum(\text{High Tide}) \quad \ldots\ldots\ldots\ldots\ldots\ldots \quad (2)$$

$$\text{Mean Low Water} = (1/N) \sum(\text{Low Tide}) \quad \ldots\ldots\ldots\ldots\ldots\ldots \quad (3)$$

$$\text{Mean Tidal Range} = \text{Mean High Water} - \text{Mean Low Water} \quad \ldots \quad (4)$$

Filtered surge data, excluding overflow values, were analyzed to produce a histogram of value distributions (Figure 4, left panel) and a graph of surge values (right panel). These analyses provide insights into the behavior of surge heights after adjusting for outliers.

The individual effects of meteorological elements—wind direction, wind speed, and atmospheric pressure—on surge height were quantified using both RGui programming software and Microsoft Excel.

RESULTS AND DISCUSSION

Previous studies have estimated monthly mean sea levels for the Eastern Mediterranean using spectral and Fourier analysis. According to data from the Permanent Service for Mean Sea Level (PSMSL), mean sea level along the Alexandria coast ranges from 67.49 to 72.76 cm (Ibrahim & El-Gindy, 2022). Another study, covering the period from 1996 to 2005, recorded minimum and maximum values of 48.62 cm and 52.96 cm, respectively. The mean sea level from 1974 to 2006 was estimated at 50.76 cm (Radwan & El-Geziry, 2013; Hendy et al., 2021).

This study analyzed 19 months of sea level data from Alexandria Western Harbor, spanning June 2018 to January 2020. The results showed an estimated mean sea level of 51.1 cm. The highest recorded sea level during the study period was 1.04 m in December 2019, while the lowest was 0.122 m in April 2019.

This analysis provides a detailed understanding of how meteorological factors influence surge behavior and sea level variations in Alexandria Western Harbor.

Analysis of the sea level data identified 69 tidal harmonic constituents, of which 37 are significant, including the four principal constituents: M2, S2, O1, and K1 (Pawlowicz et al., 2002).

The mean sea level (MSL) heights throughout the study period are depicted in Figure (5), generated using RGui software. The x-axis represents the total observation period in six-month intervals and the mean values are represented at y- axis. The green dashed line indicates the actual variable mean sea level, influenced by astronomical tidal fluctuations.

MRT
ISSN 2812-5622
http://dx.doi.org/10.21622/MRT.2025.04.1.1110

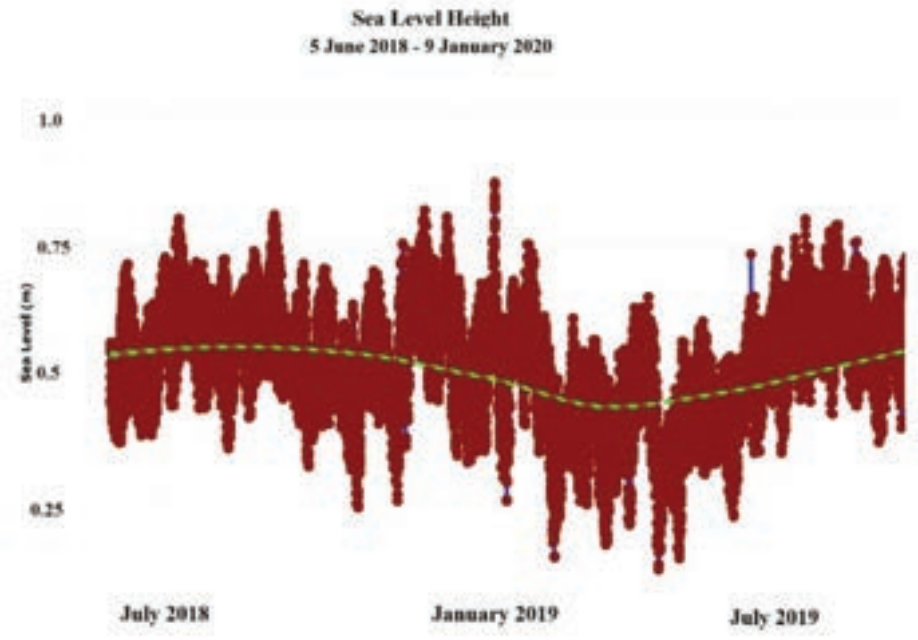

Fig. 5. Mean sea level height from 5 June 2018 – 9 January 2020

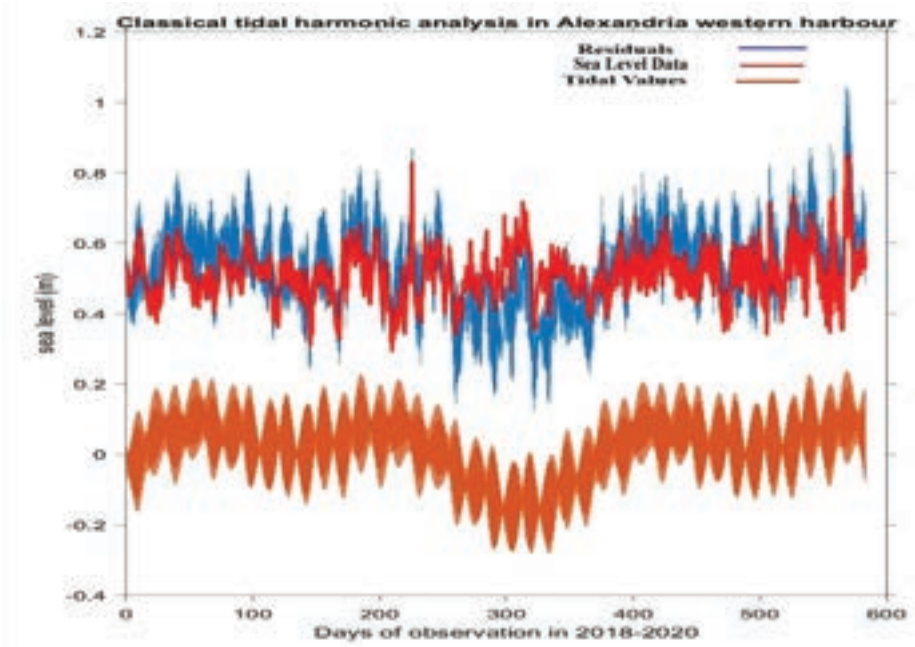

Fig. 6. Tidal signal, sea level data and residuals, and of the residuals from mean data

Table 1: Parameters of principal harmonic constituents from t-tide software analysis

Principal Harmonic Constituent	Frequency	Amplitude (cm)	Phase (φ)
M_2	0.0805114	7.24	310.38°
S_2	0.0833333	4.45	324.71°
K_1	0.0417807	1.7	310.88°
O_1	0.0387307	1.23	274.76°

The type of tide in Alexandria Western Harbor is determined by calculating the F factor, which is defined as:

$$\text{Factor} = \frac{HK_1 + HO_1}{HM_2 + HS_2} \quad \text{..... (5)}$$

(Pugh, 1987; Ozturk & Yuksel, 2023)

Where H represents the amplitude of each principal harmonic constituent (M2, S2, K1, O1).

Using the following values for the amplitudes:

K1 = 1.7 cm

O1 = 1.23 cm

M2 = 7.24 cm

S2 = 4.45 cm

The F factor is calculated as:

$$\text{Factor} = \frac{1.7 + 1.23}{7.24 + 4.45} = 0.25064$$

The tide type in Alexandria western harbor is thus Semi diurnal tide

Based on this value, the tide type in Alexandria Western Harbor is classified as semi-diurnal, characterized by two high and two low tides each day.

Table 2: Tidal semi diurnal, diurnal, and long period harmonic constituents' amplitudes

	Semi diurnal Harmonic Constituents				Diurnal Harmonic Constituents				Long Period	
Harmonic constituents	M_2	S_2	N_2	K_2	K_1	O_1	P_1	S_1	S_{SA}	S_A
Amp. (cm)	7.24	4.45	1.29	1.32	1.7	1.23	0.66	0.36	6.59	8.25
Phase (φ)	310.38°	324.71°	314.68°	323.06°	310.88°	274.76°	314.33°	254.57°	222.05°	277.7°

Shallow water significantly influences sea level data analysis. High water periods are relatively shorter than low water periods in shallow areas, as noted by the British Ministry of Defense (2008). Surge heights also tend to increase in shallow coastal regions. The cumulative amplitude of shallow water harmonic constituents, totaling 2.97 cm, includes components such as S4, MS4, MK4, MN4, M4, 2MK5, M6, 2MS6, 2MK6, M8, among others (Parker et al., 2007).

Figure 7 illustrates the semi-diurnal tidal pattern observed in Alexandria Harbor, characterized by sinusoidal fluctuations where each high water is followed by a corresponding low water throughout the study period.

The study revealed that surges conform a major part of sea level data; the surge maximum is 0.86 cm, minimum is 0.29 cm with mean height 0.51 cm, while the tidal component in Alexandria Western Harbor represents a small value of total sea level height as the maximum high-water level is 23.2 cm, while the minimum low-water level is -29.2 cm, the estimated mean tidal range is 16.57 cm.

MRT
ISSN 2812-5622
http://dx.doi.org/10.21622/MRT.2025.04.1.1110

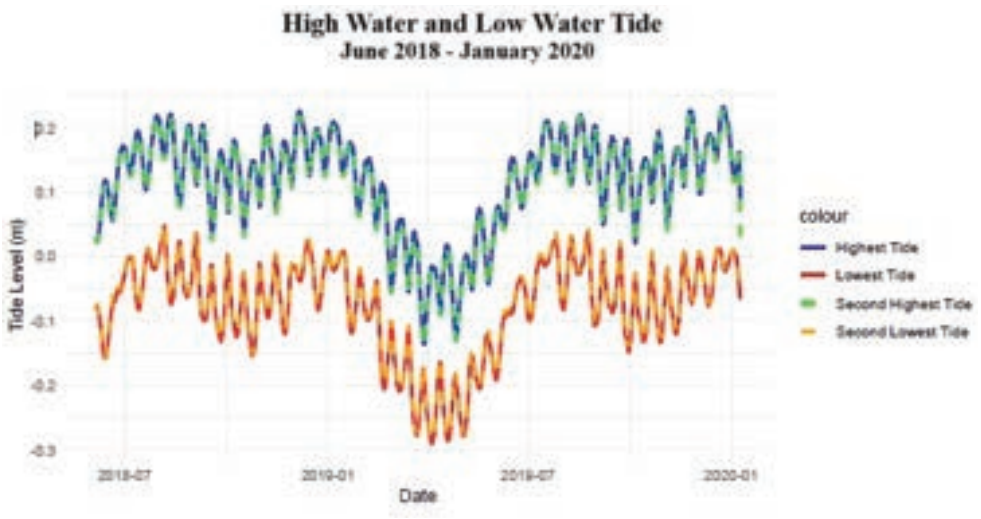

Fig. 7. High water and low water tide

The wind effect on surge height is dependent on the direction and speed of wind. The analysis of wind data exhibits the prevailing wind directions at Alexandria during the study period.

The wind effect could move the level readings from 0.1 to 0.2 meter and may reach to 0.5 meter in open coastal area (Couriel et al., 2014: Ozturk & Yuksel, 2023).

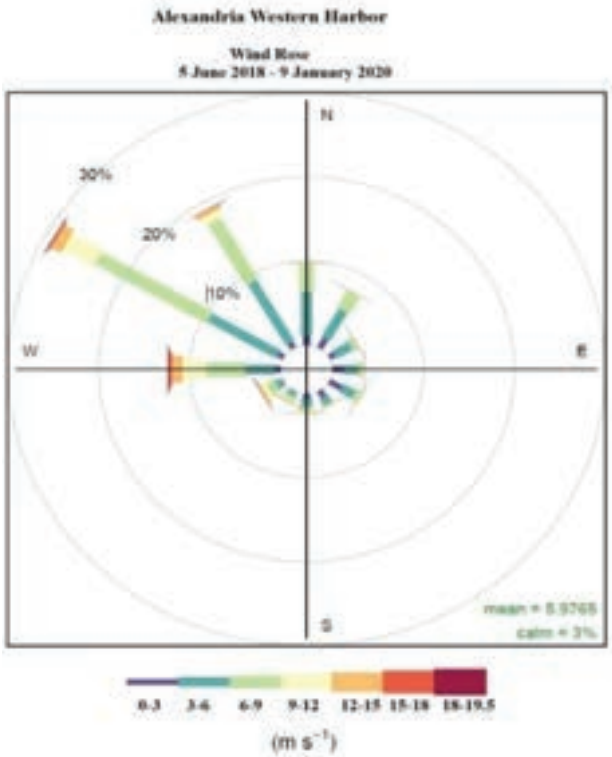

Fig. 8. Wind Rose for Alexandria Harbor

The wind data were visualized as a wind rose graphic plot (Figure 8) using RGui programming software with the OpenAir package. This plot illustrates the frequencies and directions of winds measured at the meteorological station in Ras-El Tin, Alexandria Western Harbor, over the entire 19-month observation period.

Wind directions are represented along the main and sub-cardinal axes, with the spokes indicating the frequency of wind occurrence in each direction, normalized to a total of 100% for all directions. The longest spokes, pointing towards the NW, WNW, and W directions, indicate that the prevailing winds originated primarily from the northwest quadrant during the study period. Specifically:

- 28% of the total observations recorded wind from the NW direction.
- 18% and 13% originated from the WNW and W directions, respectively.
- Wind from the N and NNE directions accounted for 10% and 8%, respectively.
- Other directions (NE, ENE, SE, S, SW) exhibited minimal wind frequencies, collectively contributing 28% of total wind occurrences.

An analysis of wind speeds reveals that the majority ranged between 3 to 9 m/s, with occasional increases to 9–12 m/s. Wind speeds rarely exceeded 15–19 m/s, primarily in the W and NW directions. The average wind speed over the observation period was 5.96 m/s, with calm periods (wind speeds below 0.5 m/s) recorded only 3% of the time.

Table 3 presents the mathematical features of monthly surge data for the study period, including maximum,

MRT
ISSN 2812-5622
http://dx.doi.org/10.21622/MRT.2025.04.1.1110

minimum, average, and median values. The study further investigates the monthly relationship between surge data and meteorological parameters over the sequential 19-month period, spanning June 2018 to December 2019.

Table 3: The monthly values of (Max., Min., Average, and Median Surge data values)

Function	Jun. 2018	Jul. 2018	Aug. 2018	Sep. 2018	Oct. 2018	Nov. 2018	Dec. 2018	Jan. 2019	Feb. 2019	Mar. 2019	Apr. 2019	May 2019	Jun. 2019	Jul. 2019	Aug. 2019	Sep. 2019	Oct. 2019	Nov. 2019	Dec. 2019
Max. (cm)	67.4	62.7	59.7	62.4	56.3	64.1	64.5	67.5	62.9	66.9	68.0	60.2	62.1	67.0	67.7	63.5	67.4	67.8	67.9
Min. (cm)	38.5	43.2	41.8	37.8	32.0	31.8	29.2	30.2	33.4	40.4	35.4	38.6	37.9	42.9	42.8	34.8	34.0	38.2	35.0
Aver. (cm)	49.6	53.1	50.5	52.5	47.1	48.9	50.9	46.1	48.7	50.7	54.8	50.8	48.0	52.3	51.4	50.7	52.0	55.3	50.9
Median (cm)	48.3	53.0	50.1	52.7	48.3	49.5	51.8	44.4	48.3	49.8	57.0	50.9	47.8	51.9	50.7	52.5	52.3	55.5	50.1

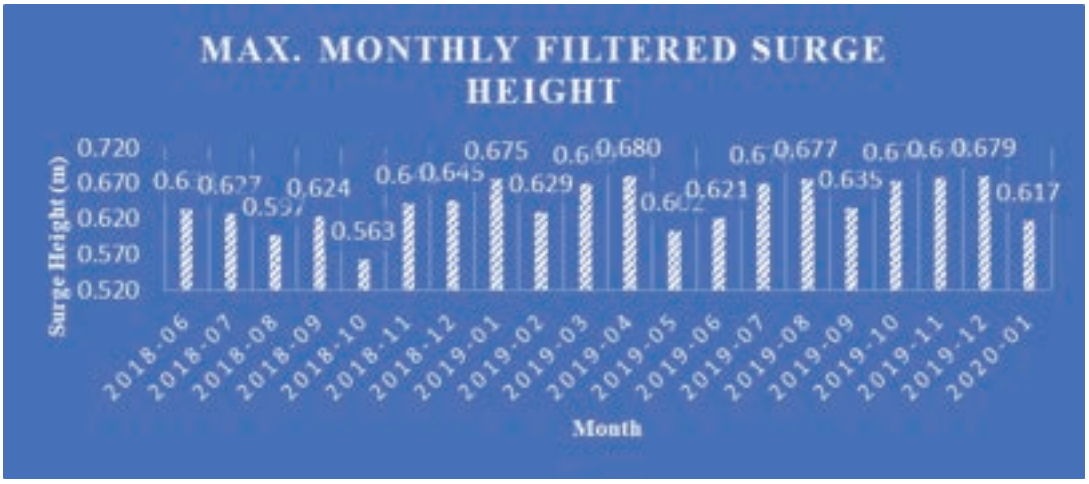

Fig. 9. Max. monthly filtered surge

The maximum filtered surge height during the study period was 0.68 m in April 2019, while the maximum unfiltered surge height reached 0.864 m in December 2019.

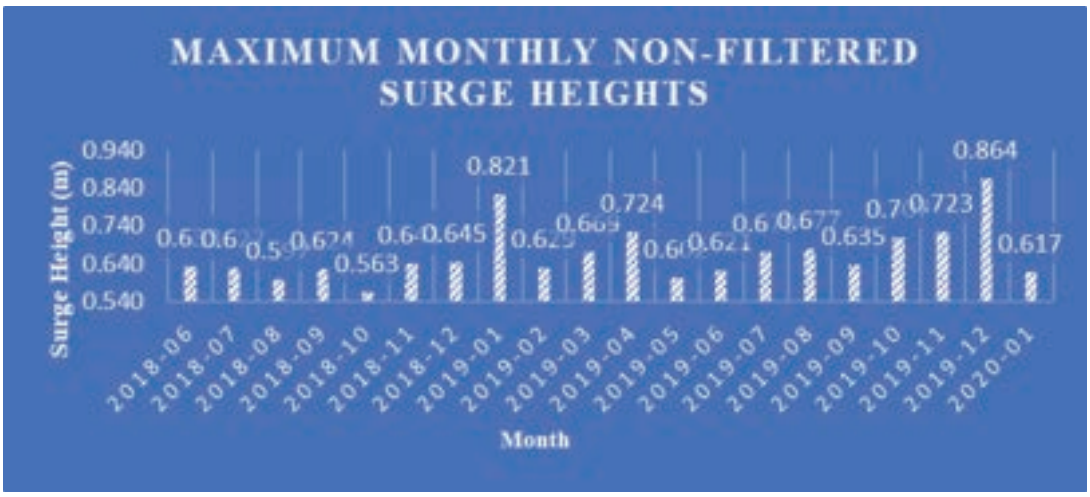

Fig. 10. Max. monthly non-filtered surge heights

MRT
ISSN 2812-5622
http://dx.doi.org/10.21622/MRT.2025.04.1.1110

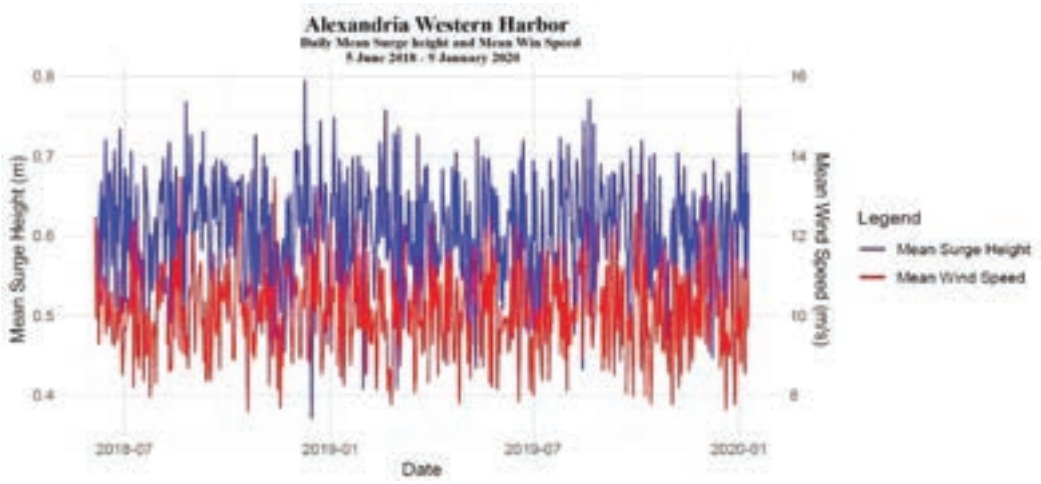

Figure 11. Mean surge heights and wind speed

Significant monthly variations in surge height were observed, particularly in November 2018, January 2019, February 2019, and April 2019. Analysis of meteorological parameters during these months revealed notable correlation factors with wind direction and atmospheric pressure. For instance:

- January 2019: Wind speed correlation factor (0.3), wind direction (0.29), and air pressure (-0.5).
- December 2018: The highest correlation between wind speed and surge height (0.56), though wind direction correlation was lower (0.27). Winds were predominantly from the west to northwest, and atmospheric pressure exhibited a high inverse correlation (-0.5).

The highest filtered surge value of 0.68 m occurred in April 2019 (Figure 10), specifically on April 8, 9, 14, 15, and 16. During this period, wind speeds ranged from 4.1 to 11.8 m/s, predominantly from W, NW, and NNW directions, while air pressure remained relatively low at 1005.5 to 1010.6 mb (Table 4).

Table 4: Highest surge values and meteorological factors in April 2019

Date	Surge (m)	Wind dir.	Wind Speed (m/s)	Pressure (mb) (mb)
08/04/2019	0.67	330°	4.1	1007.6
08/04/2019	0.67	350°	4.1	1007.2
08/04/2019	0.68	020°	4.1	1007
09/04/2019	0.68	260°	6.2	1006.6
09/04/2019	0.68	280°	6.2	1006.6
09/04/2019	0.67	270°	6.7	1006.6
09/04/2019	0.66	280°	8.7	1007.4
09/04/2019	0.65	290°	10.3	1008.3
14/04/2019	0.68	280°	10.3	1009.4
14/04/2019	0.66	270°	9.3	1010.0
16/04/2019	0.66	260°	7.2	1011
16/04/2019	0.67	260°	9.3	1010.6
16/04/2019	0.68	300°	11.8	1010.6

In contrast, the lowest surge value of 0.3 m was recorded in December 2018. During this time, wind speeds ranged from 0 to 12 m/s, with wind directions mainly from S, SW, and SSE, and air pressure values between 1020.1 and 1016.8 mb (Table 5).

Table 5: Lowest surge values and meteorological factors occurred in December 2018

Date	Surge (m)	Wind dir.	Wind Speed (m/s)	Pressure (mb) (mb)
31/12/2018	0.33	180	4	1020.1
31/12/2018	0.33	240	10	1018.4
31/12/2018	0.32	240	12	1017.2
31/12/2018	0.31	260	12	1017
31/12/2018	0.31	270	7	1017
31/12/2018	0.30	270	5	1016.8
31/12/2018	0.29	0	0	1016.8
31/12/2018	0.29	150	4	1017.4
31/12/2018	0.30	0	0	1017.5

The results indicate that surge heights are most strongly correlated with wind speed and westerly wind directions, while an inverse correlation exists with atmospheric pressure. The overall correlation

coefficients for the entire study period were:

- Surge and wind speed: (0.25).
- Surge and wind direction: (0.158).
- Surge and atmospheric pressure: (-0.35).

Monthly analysis confirmed that prevailing northwesterly winds along Alexandria's coast significantly influenced high surge levels. Higher wind speeds in the northwesterly direction were associated with greater surge heights, while increased atmospheric pressure corresponded to lower surge heights.

The effects of meteorological factors on surge heights are illustrated in the regression plots:

- Figure 13: Relationship between surge and wind speed.
- Figure 14: Relationship between surge and wind direction.
- Figure 15: Relationship between surge and atmospheric pressure.

Surge heights at any given time are primarily determined by the combined effects of wind speed, wind direction, and atmospheric pressure. Months with low or inverse correlations, such as August 2018 (wind speed correlation: 0.004), April 2019 (wind speed correlation: -0.05), and September 2019 (wind speed correlation: -0.15), also showed low correlations for wind direction (-0.07, 0.17, and -0.07), while the correlation with atmospheric pressure was higher (inversely proportional) at (-0.4, -0.6, and -0.6), respectively.

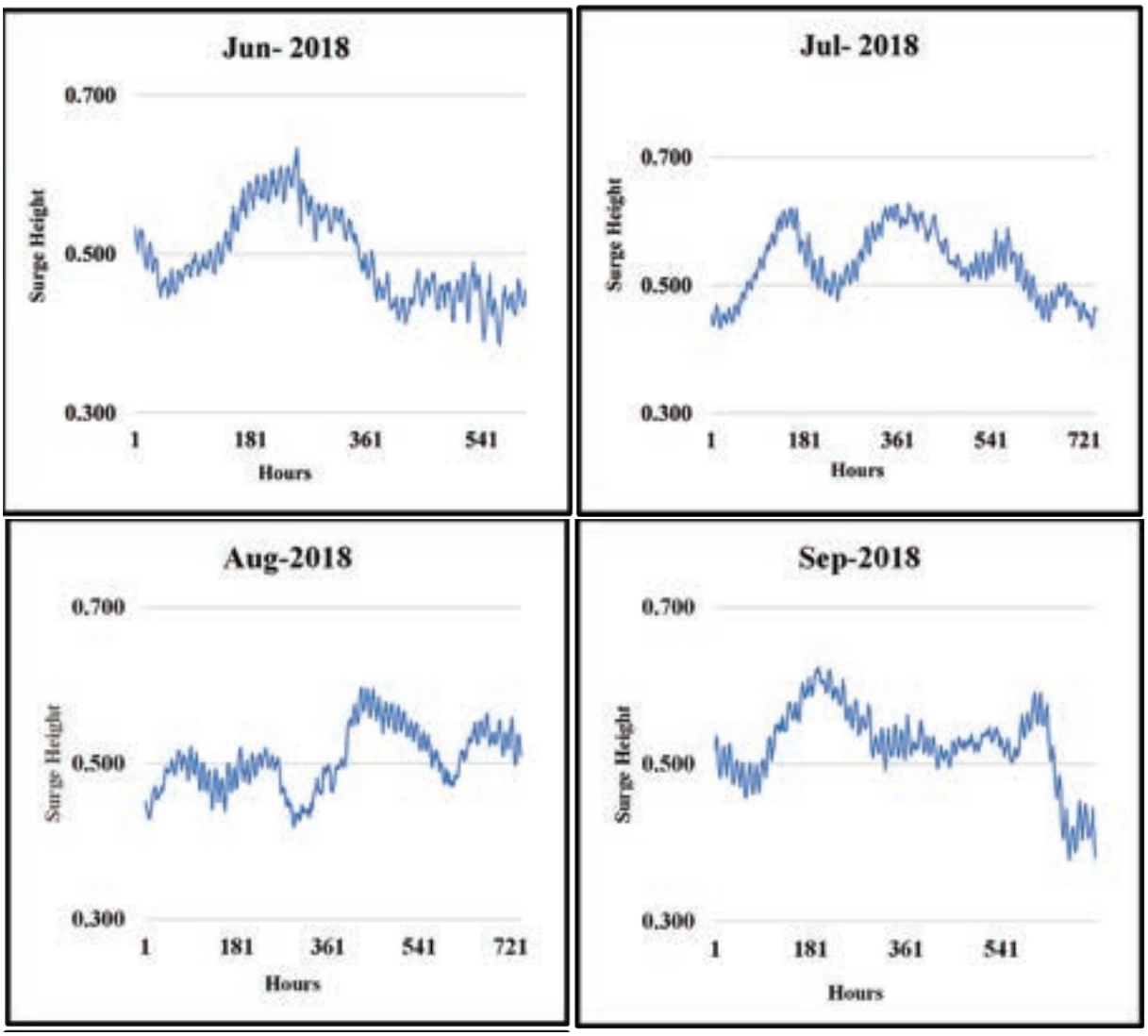

MRT
ISSN 2812-5622
http://dx.doi.org/10.21622/MRT.2025.04.1.1110

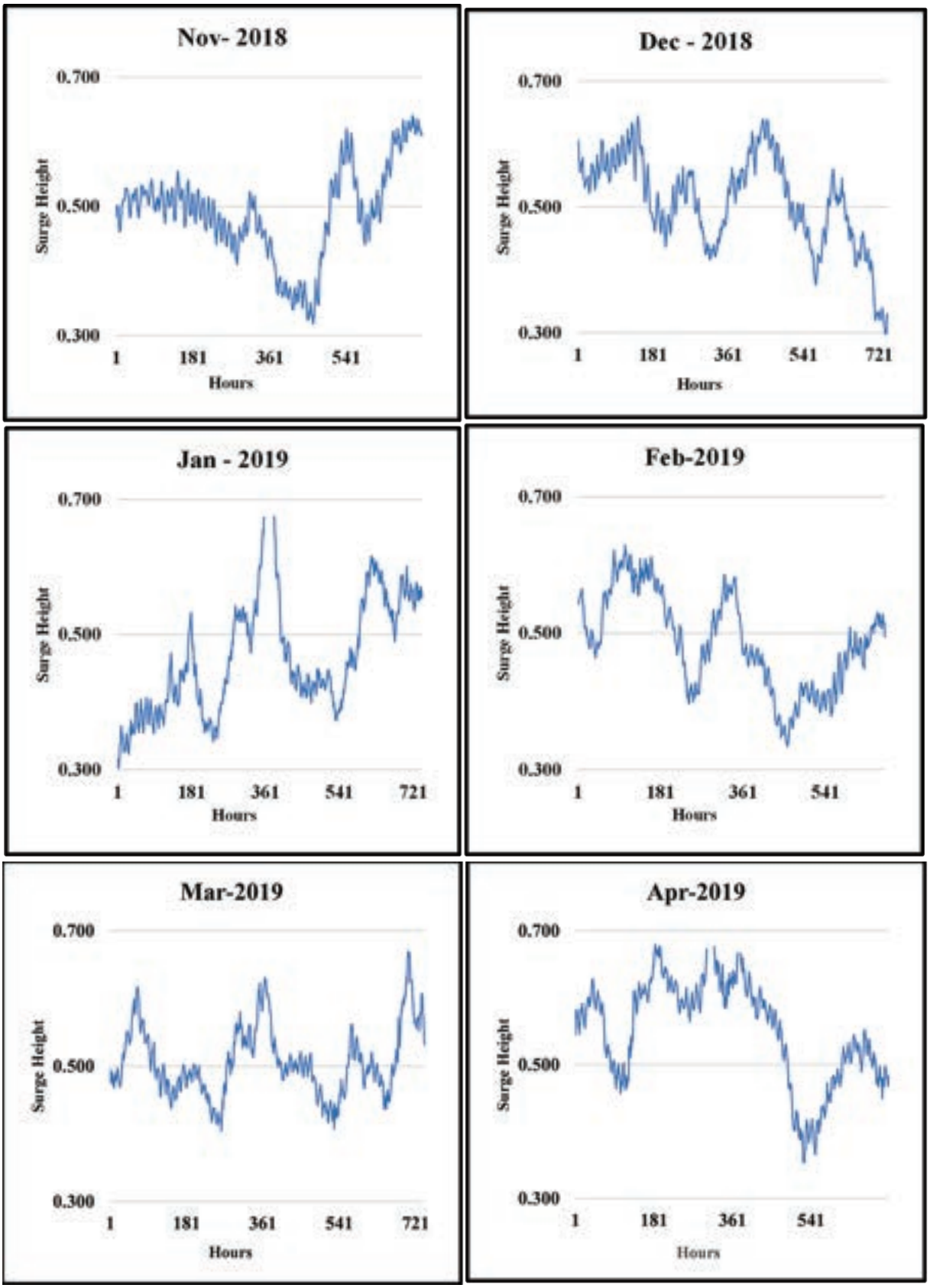

MRT
ISSN 2812-5622
http://dx.doi.org/10.21622/MRT.2025.04.1.1110

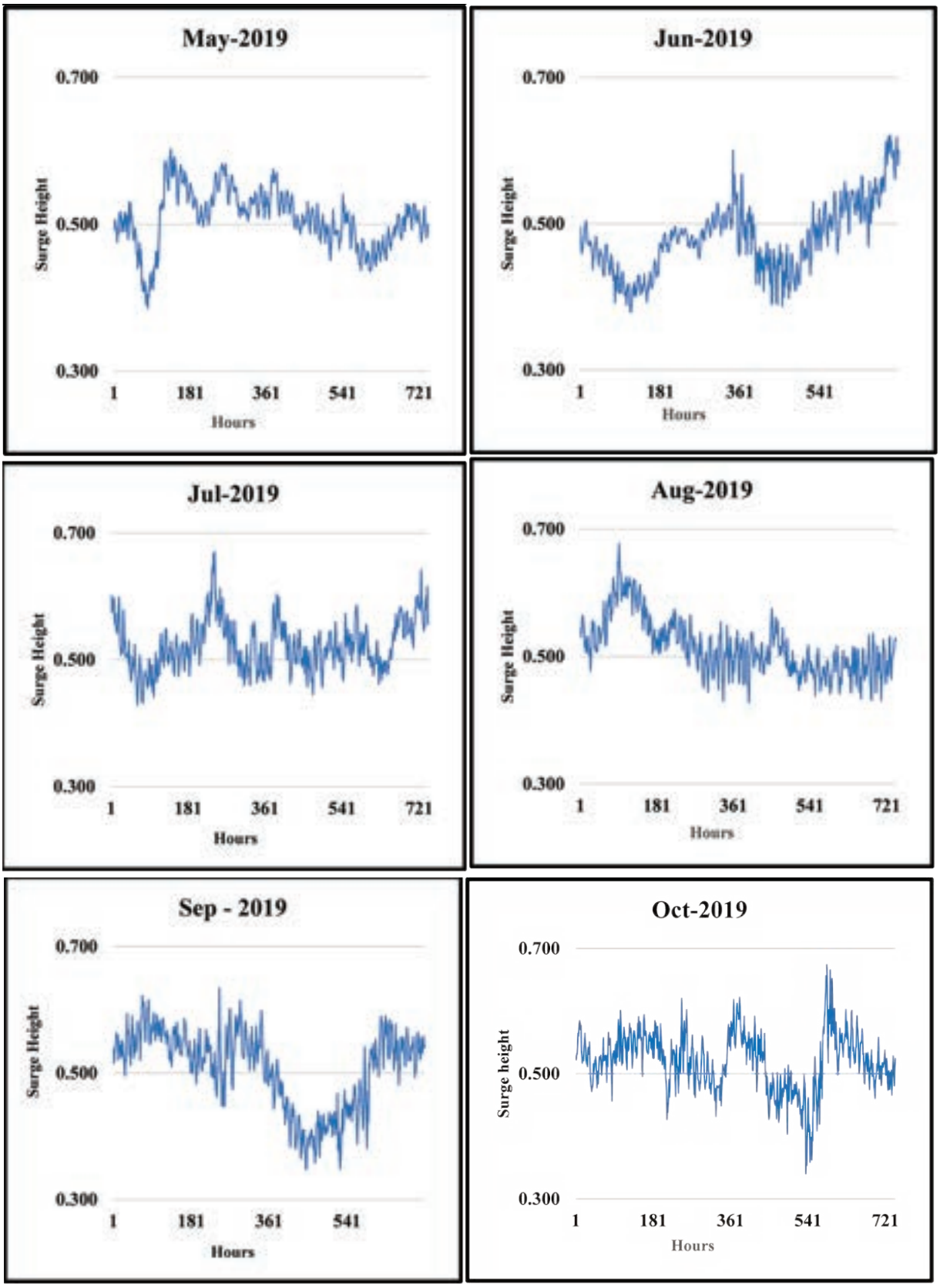

MRT
ISSN 2812-5622
http://dx.doi.org/10.21622/MRT.2025.04.1.1110

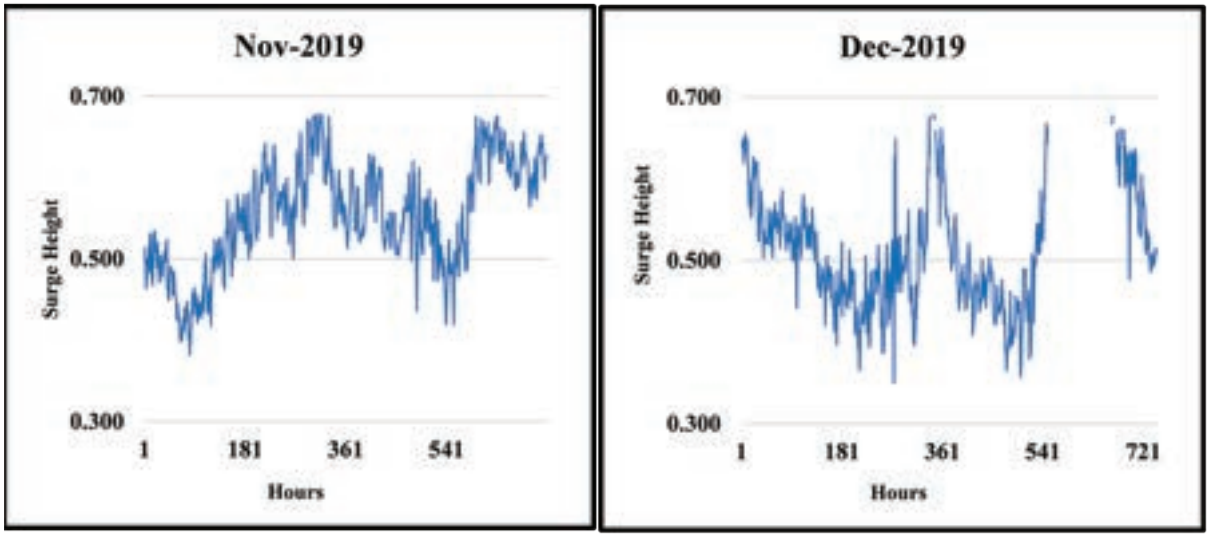

Fig. 12. The Monthly changes in Filtered Surge Heights

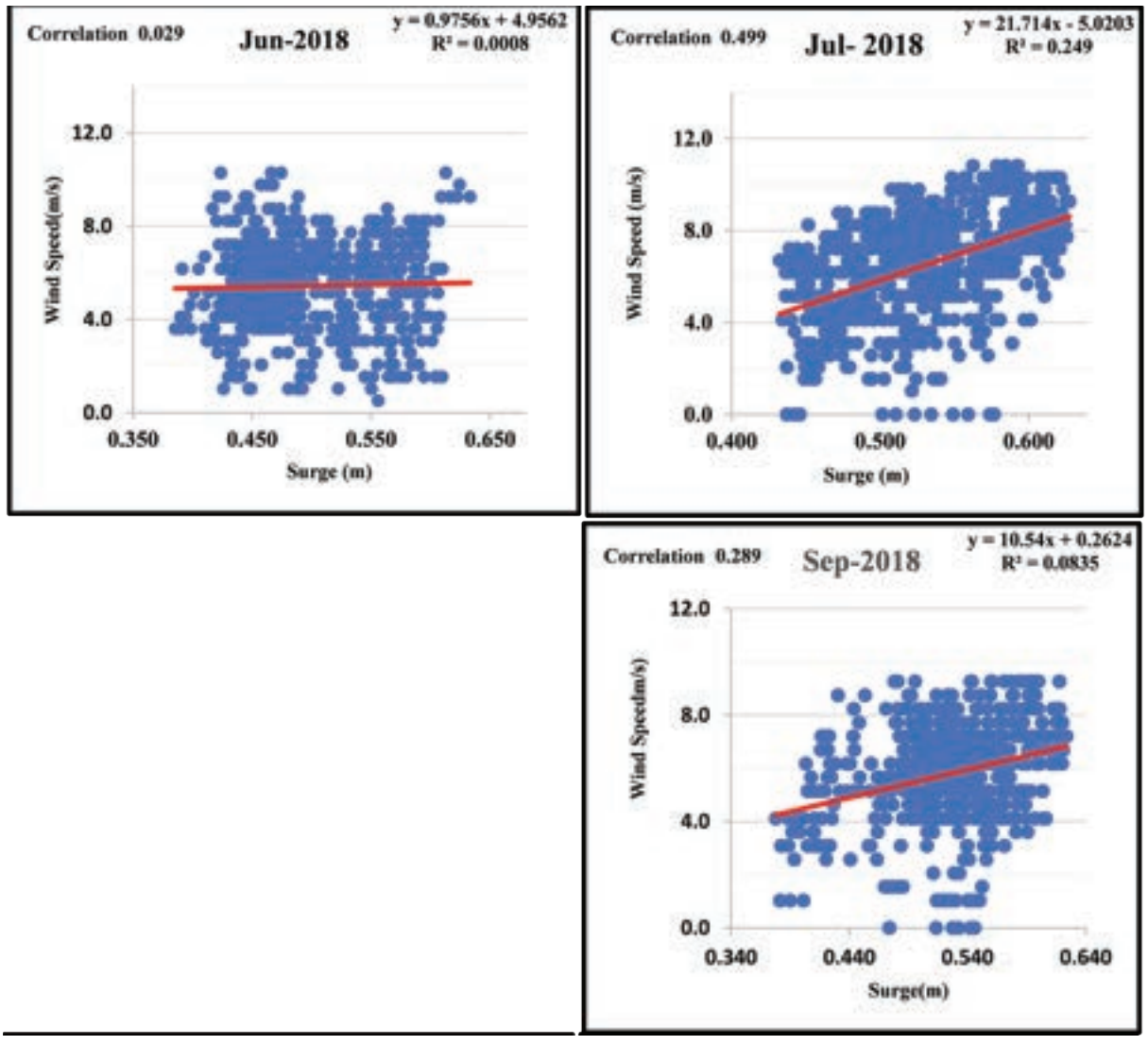

MRT
ISSN 2812-5622
http://dx.doi.org/10.21622/MRT.2025.04.1.1110

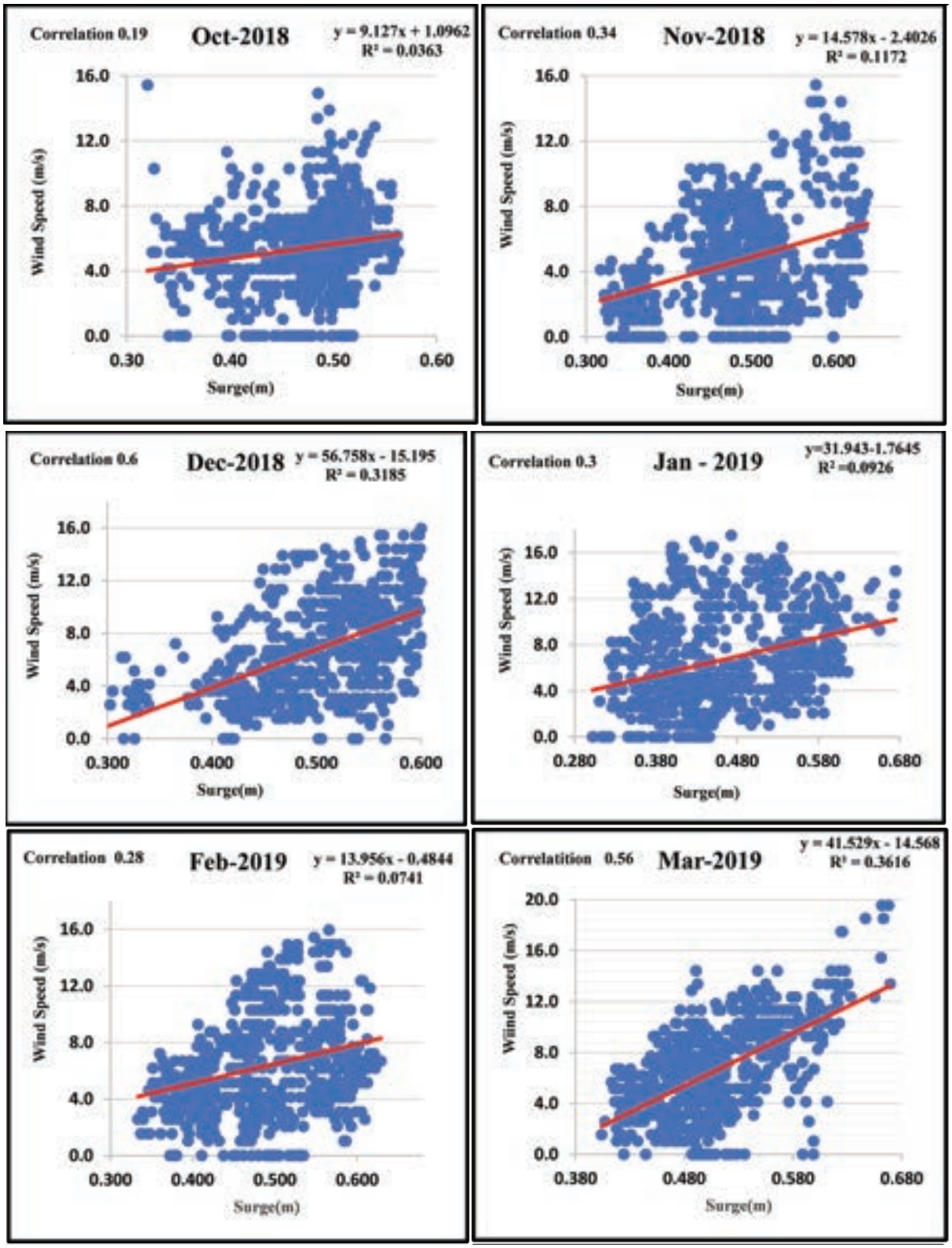

MRT
ISSN 2812-5622
http://dx.doi.org/10.21622/MRT.2025.04.1.1110

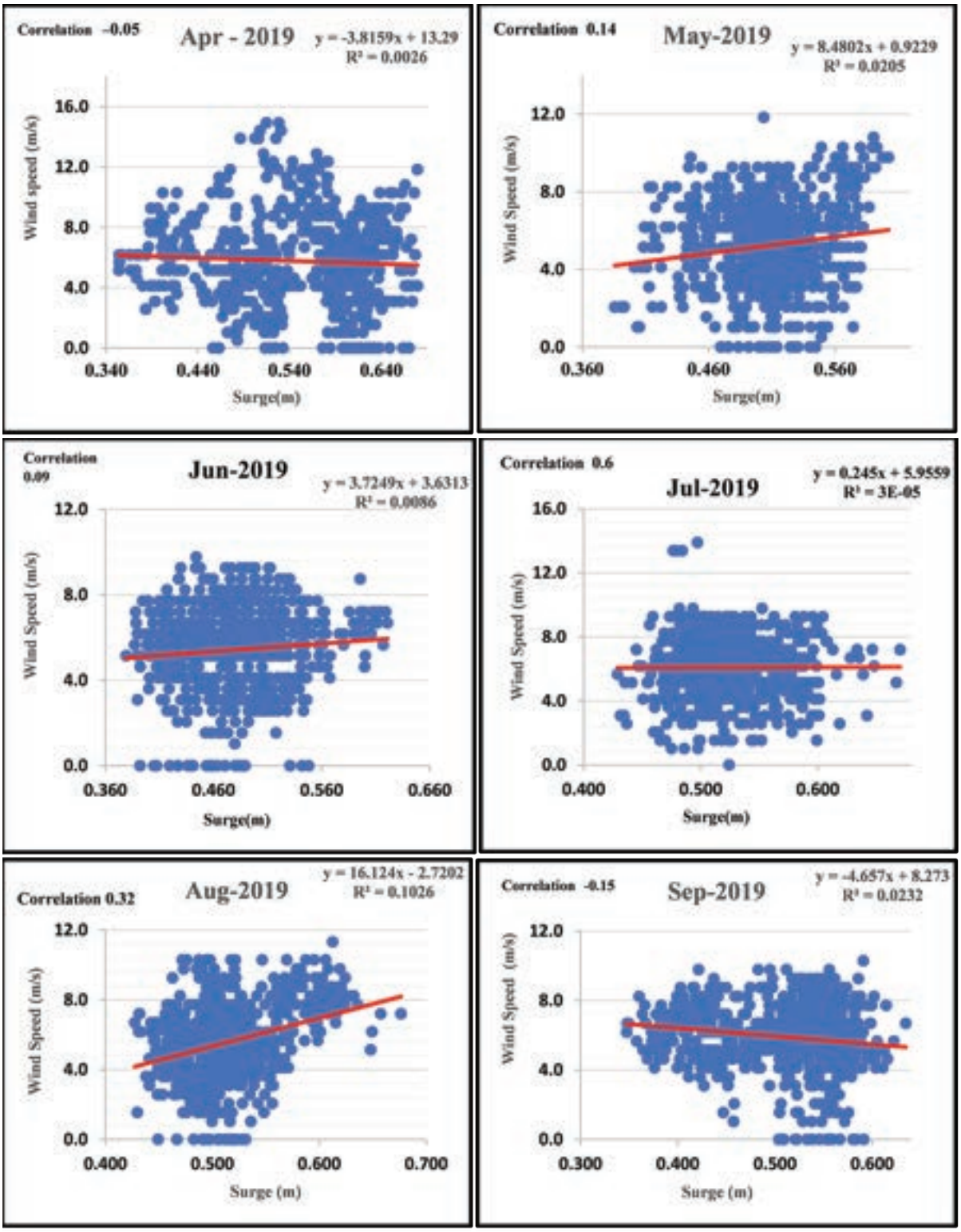

MRT
ISSN 2812-5622
http://dx.doi.org/10.21622/MRT.2025.04.1.1110

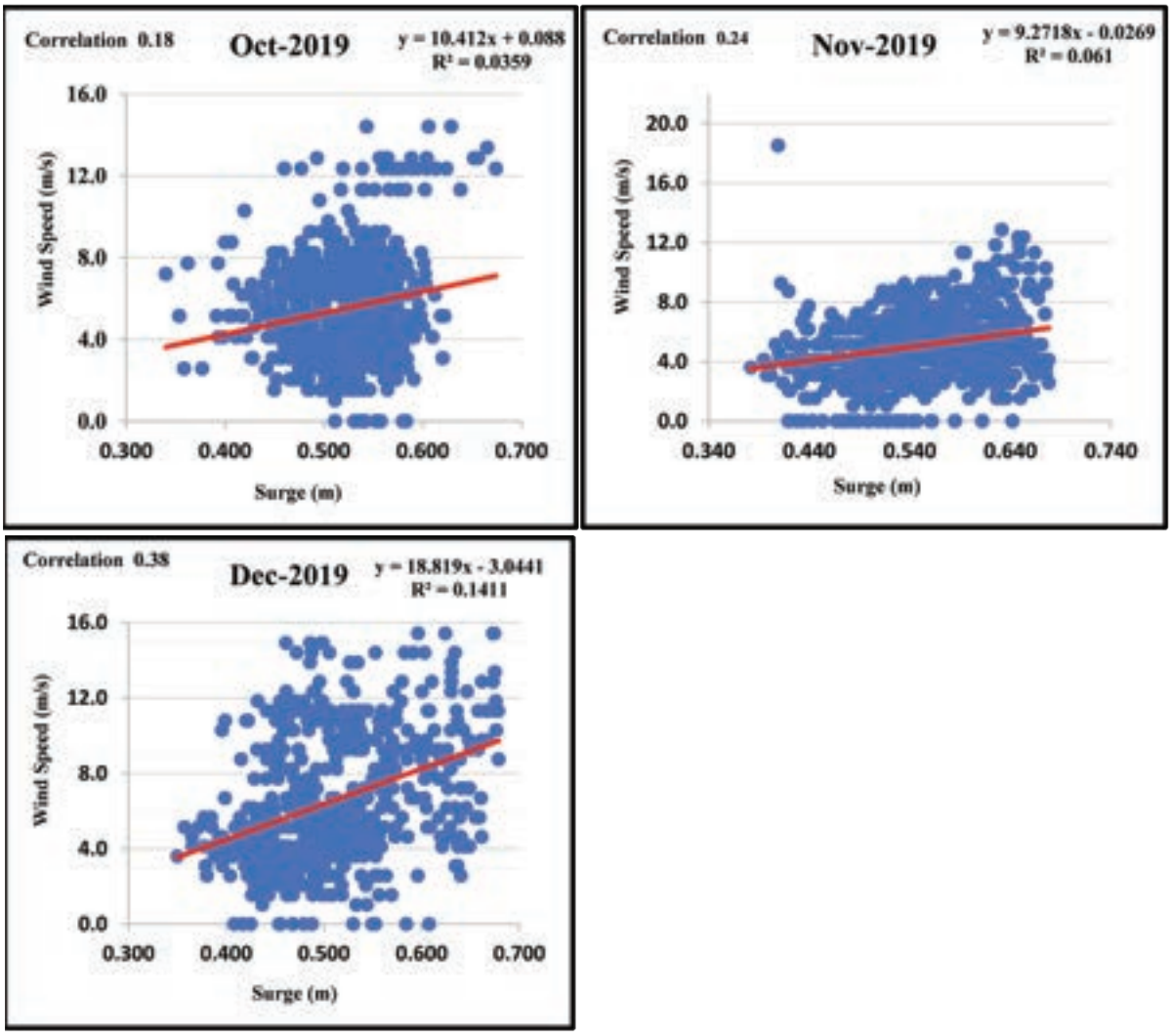

Fig. 13. The Correlation between Surge data and Wind Speed

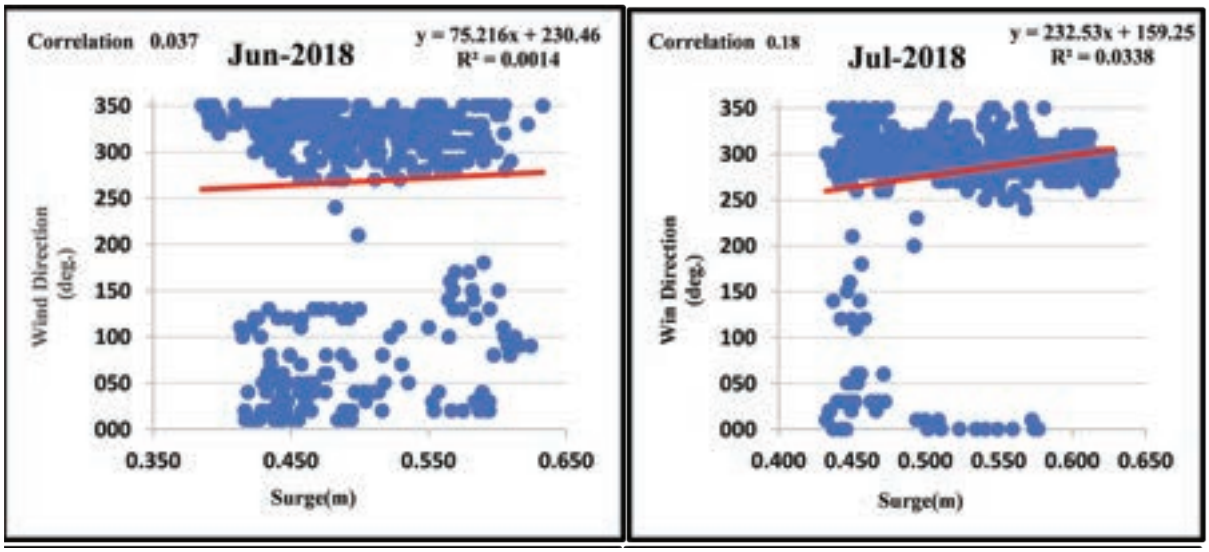

MRT
ISSN 2812-5622
http://dx.doi.org/10.21622/MRT.2025.04.1.1110

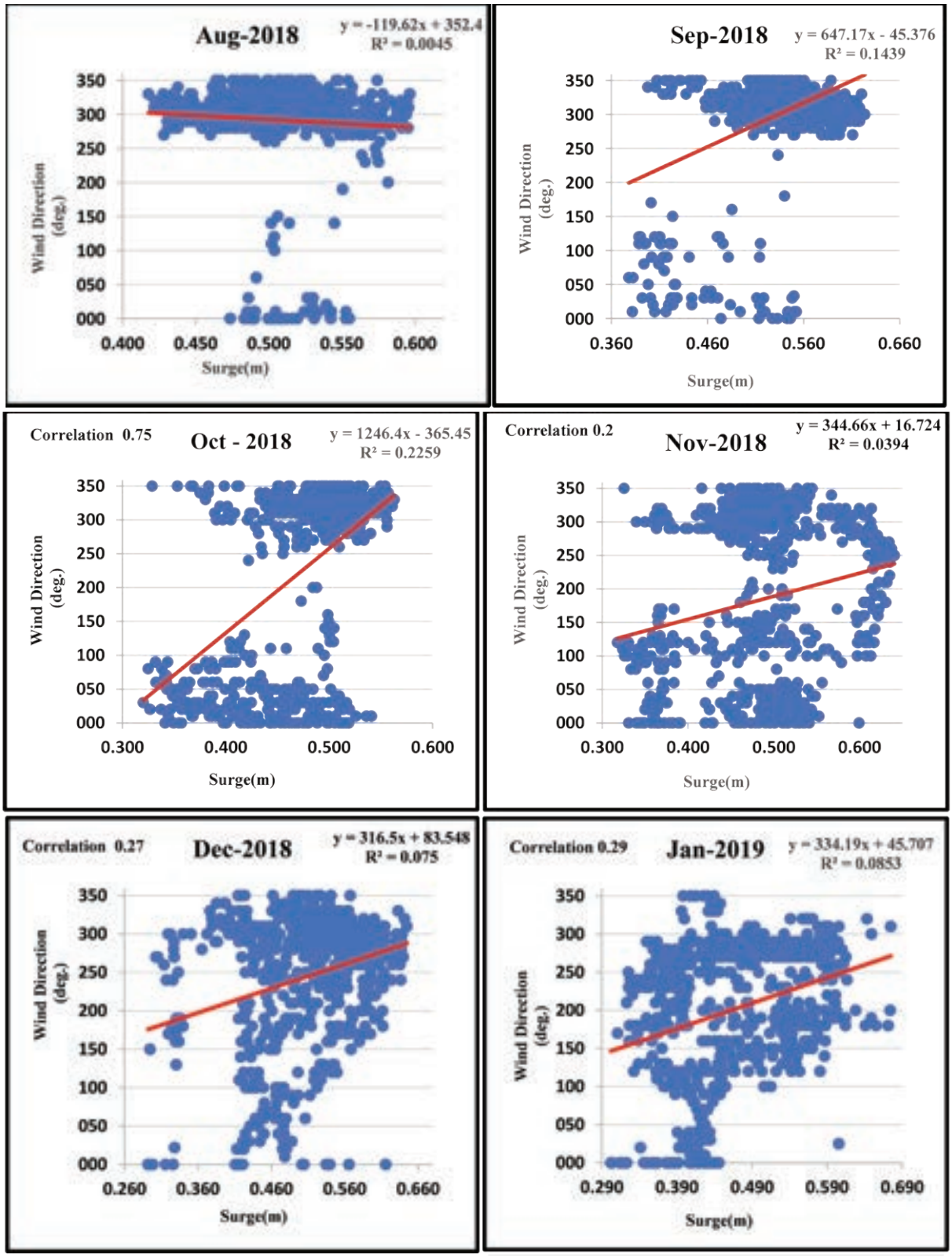

MRT
ISSN 2812-5622
http://dx.doi.org/10.21622/MRT.2025.04.1.1110

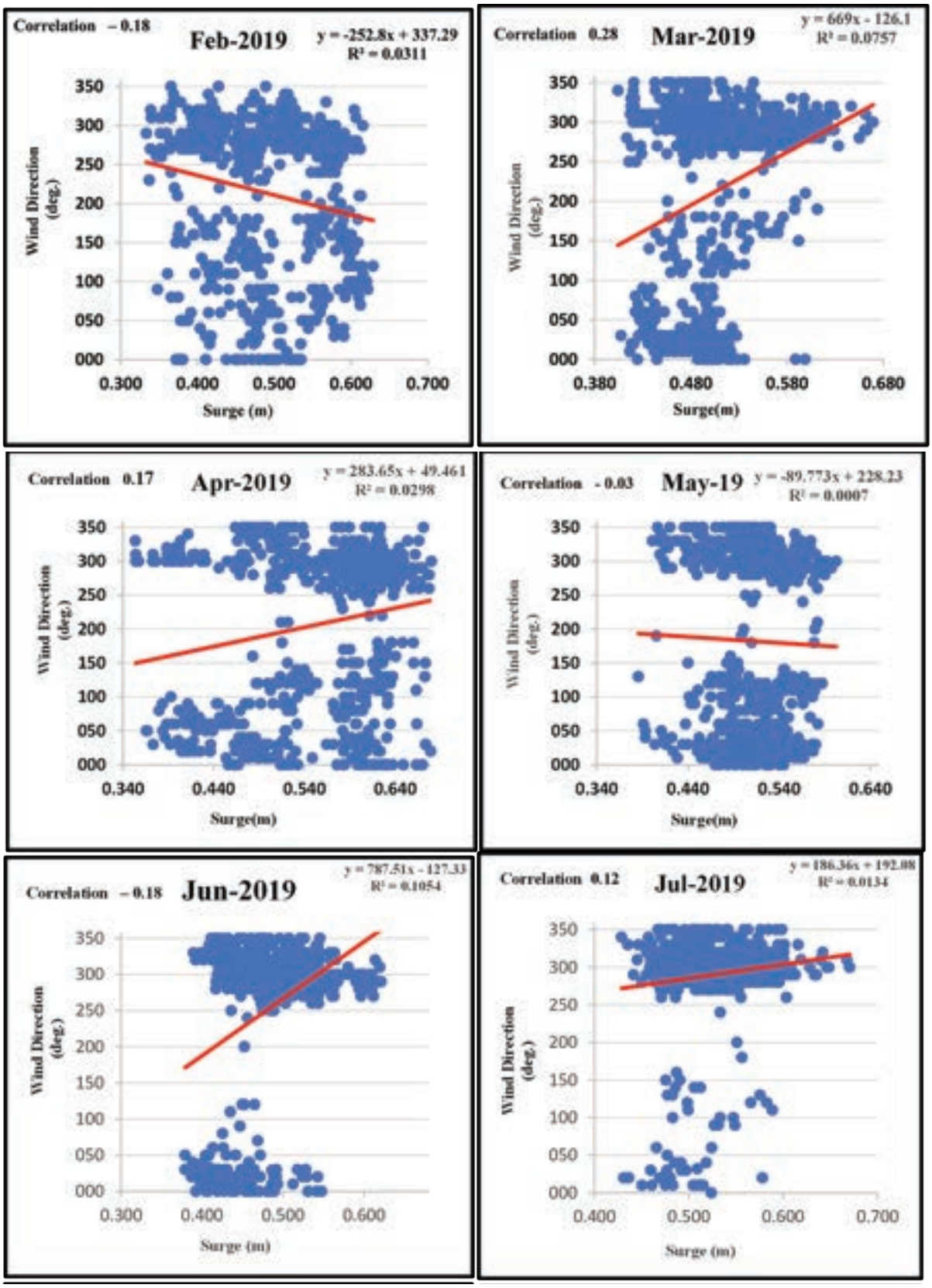

MRT
ISSN 2812-5622
http://dx.doi.org/10.21622/MRT.2025.04.1.1110

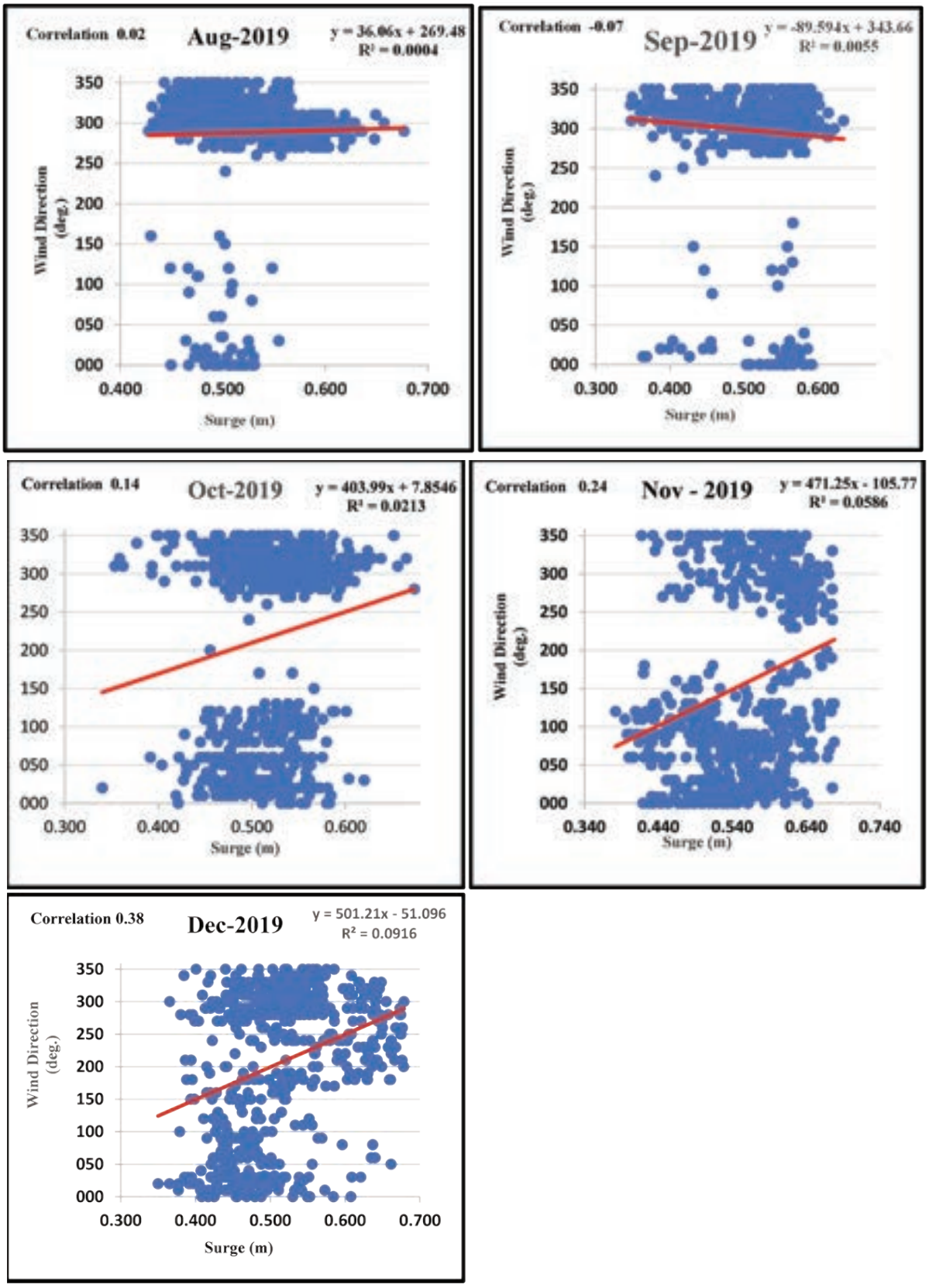

Fig. 14. The correlation between Surge data and Wind Direction

MRT
ISSN 2812-5622
http://dx.doi.org/10.21622/MRT.2025.04.1.1110

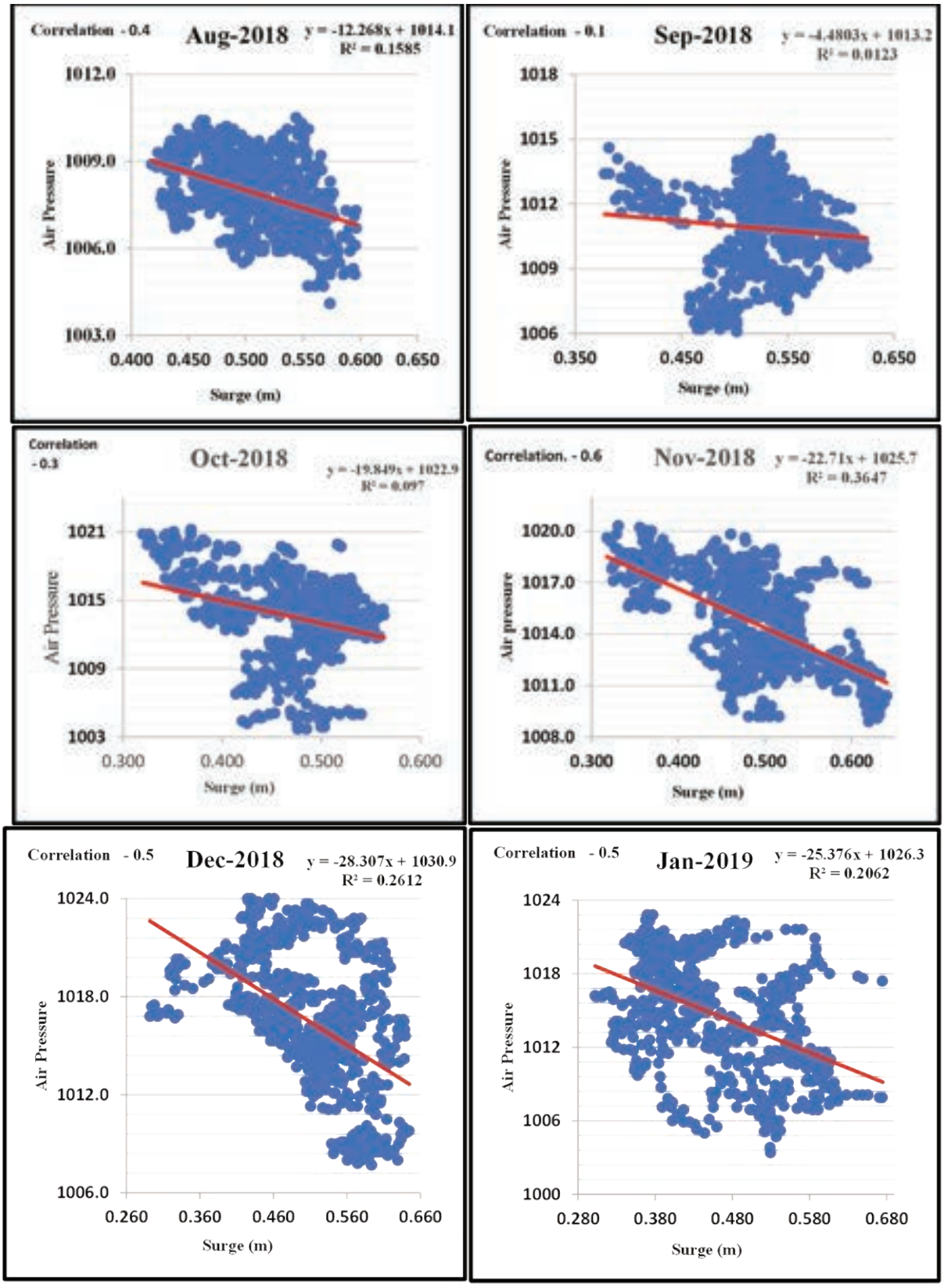

MRT
ISSN 2812-5622
http://dx.doi.org/10.21622/MRT.2025.04.1.1110

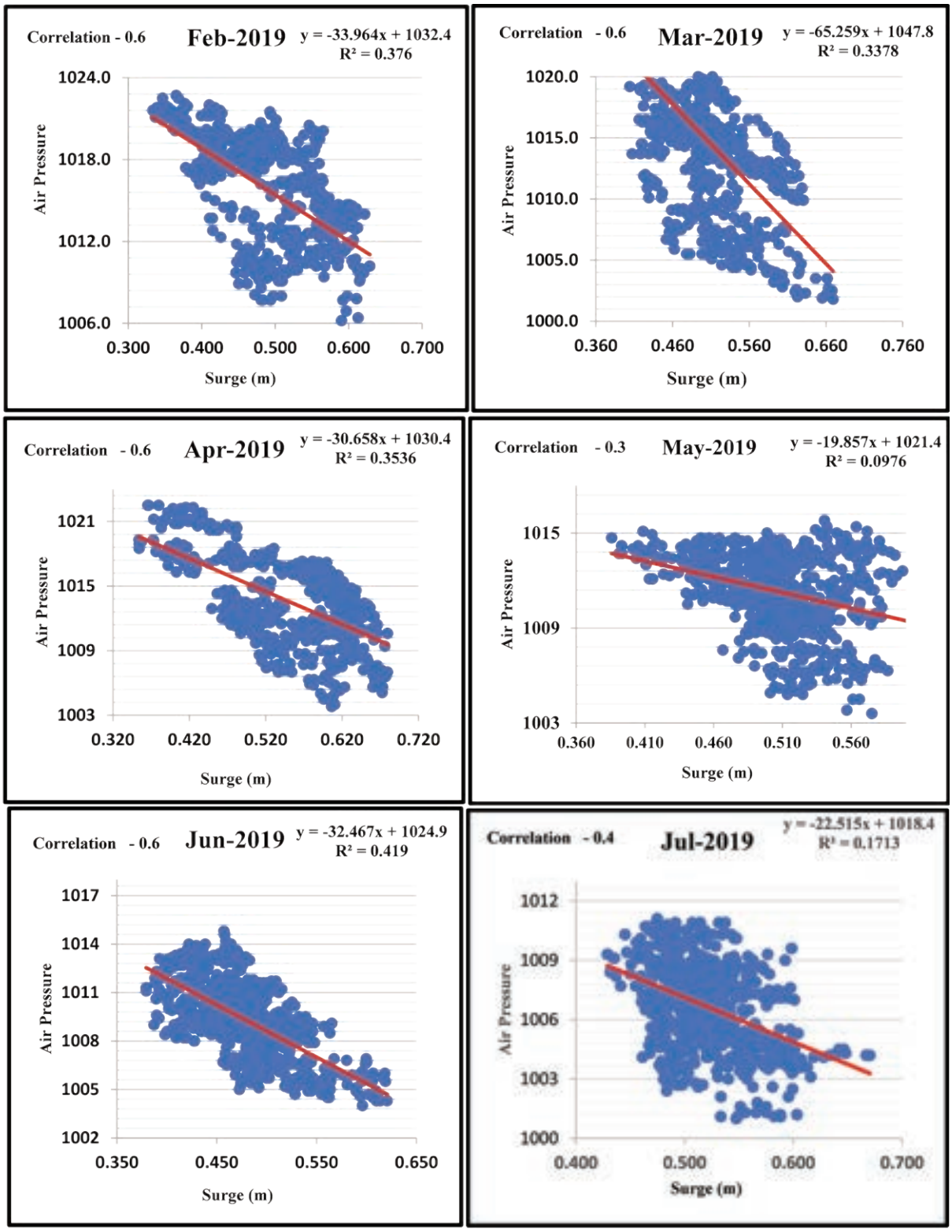

MRT
ISSN 2812-5622
http://dx.doi.org/10.21622/MRT.2025.04.1.1110

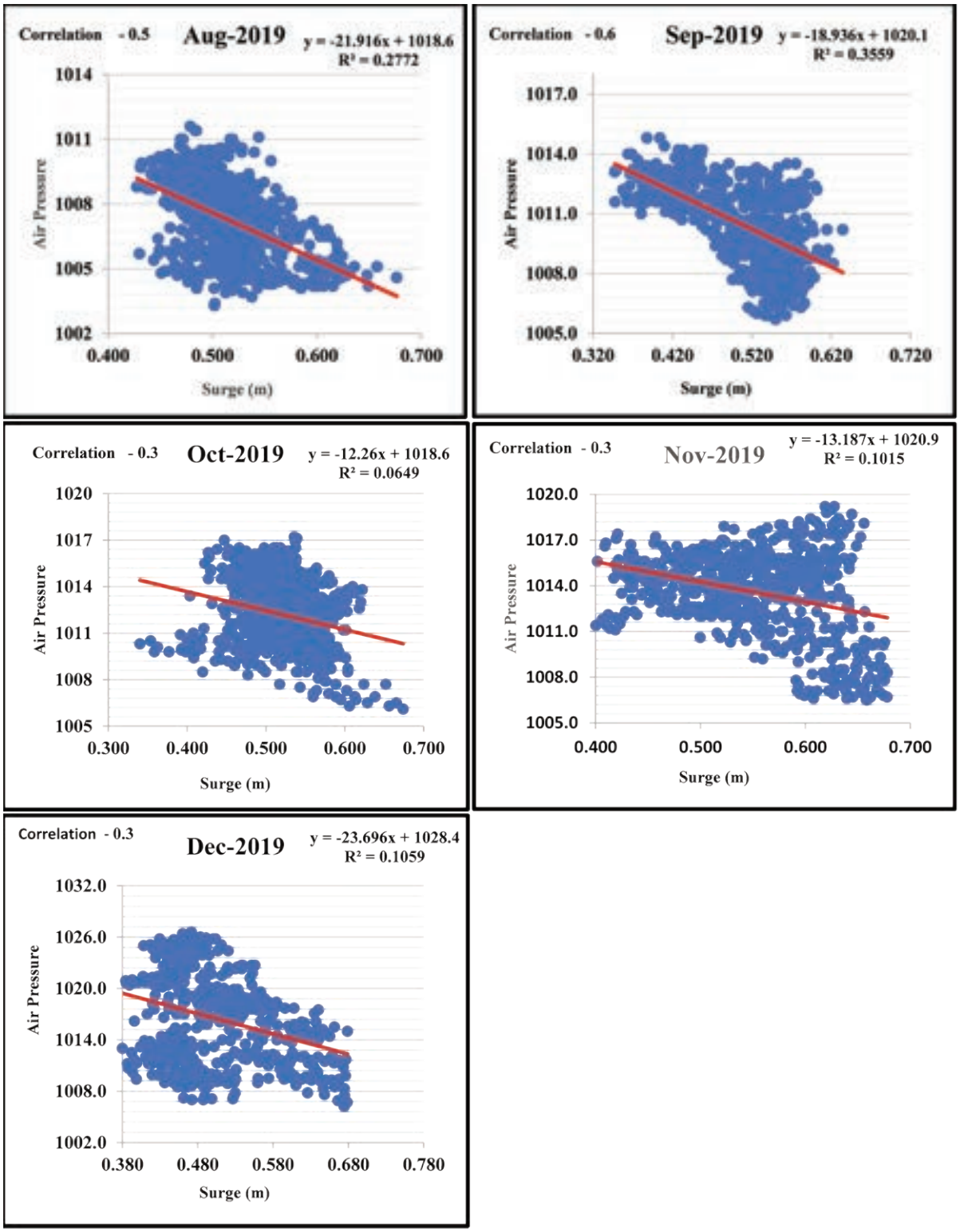

Fig. 15. The relation between Surge data and Air Pressure

MRT
ISSN 2812-5622
http://dx.doi.org/10.21622/MRT.2025.04.1.1110

CONCLUSION

Sea level rise is one of the most critical global challenges, threatening coastal regions worldwide with inundation. Alexandria, Egypt, is among the vulnerable areas, with surges accounting for more than two-thirds of total sea level height.

This study highlights the influence of meteorological factors as wind speed, wind direction, and atmospheric pressure on surge variations in Alexandria Harbor throughout the year. Seasonal changes in atmospheric pressure and air fronts over the southern Mediterranean, coupled with prevailing winds, govern surge heights. Timely implementation of appropriate measures, based on scientific analysis of surge timing and heights, is essential to safeguard Alexandria's coast from potential flooding and reduce the cost of post-flood recovery efforts.

The ability to accurately determine sea level variations is crucial for effective coastal management, oceanography applications, and environmental protection. Alexandria, like many other global coastal regions, is highly susceptible to flooding and the impacts of sea level rise. High surge values, particularly during storms, exacerbate coastal erosion, flooding, infrastructure damage, and environmental degradation.

To mitigate these risks, proactive measures are required. Constructing protective structures such as seawalls and levees is an urgent necessity. Additionally, preserving natural barriers like mangroves and sand dunes can offer significant protection to coastal areas particularly bared land at Abo Quir in the eastern section of the city.

Relocation of communities and infrastructure from probable vulnerable areas in Alexandria and restoration of coastal ecosystems to enhance natural resilience against sea level rise and storm surges considered significant strategies for climate adaptation in Alexandria.

By implementing these measures, Alexandria could be better adapted to the ongoing challenges posed by climate change and can protect its coastal environments and communities.

REFERENCES

Andrée, E. *et al.* (2022) 'Simulating wind-driven extreme sea levels: Sensitivity to wind speed and direction', *Weather and Climate Extremes*, 36, p. 100422. Available at: https://doi.org/10.1016/j.wace.2022.100422.

Baldan, D. *et al.* (2023) 'Return periods of extreme sea levels: From magnitude to frequency, duration and seasonality. Implications in a regulated coastal lagoon', *Science of The Total Environment*, 866, p. 161326. Available at: https://doi.org/10.1016/j.scitotenv.2022.161326.

Church, J.A. and White, N.J. (2011) 'Sea-Level Rise from the Late 19th to the Early 21st Century', *Surveys in Geophysics*, 32(4–5). Available at: https://doi.org/10.1007/s10712-011-9119-1.

Couriel, E., Modra, B. and Jacobs, R. (2014) 'NSW Sea Level Trends – The Ups and Downs', in *Australian Hydrographers Association Conference*.

El-Geziry, T.M. (2013) 'General pattern of sea level variation in front of Alexandria (Egypt) and its relationship to the wind pattern', *Egyptian Journal of Aquatic Research*, 39(3). Available at: https://doi.org/10.1016/j.ejar.2013.10.002.

El-Geziry, T.M. and Said, M.A. (2020) 'Spatial Variations of Sea Level along the Egyptian Mediterranean Coast', *ATHENS JOURNAL OF MEDITERRANEAN STUDIES*, 6(2). Available at: https://doi.org/10.30958/ajms.6-2-3.

'Fleet Publications and Graphics Organisation. Admiralty manual of navigation: Volume 1 – The principles of navigation (10th ed.). ' (2008) *The Nautical Institute. Published with permission of the Controller of Her Majesty's Stationery Office.* [Preprint].

Frihy, O.E. (1992) 'Sea-level rise and shoreline retreat of the Nile Delta promontories, Egypt', *Natural Hazards*, 5(1). Available at: https://doi.org/10.1007/BF00127140.

Gomis, D. *et al.* (2008) 'Low frequency Mediterranean sea level variability: The contribution of atmospheric pressure and wind', *Global and Planetary Change*, 63(2–3), pp. 215–229. Available at: https://doi.org/10.1016/j.gloplacha.2008.06.005.

Gumuscu, I. *et al.* (2024) 'Evaluation of future wind climate over the Eastern Mediterranean Sea', *Regional Studies in Marine Science*, 78, p. 103780. Available at: https://doi.org/10.1016/j.rsma.2024.103780.

Hdidouan, D. and Staffell, I. (2017) 'The impact of climate change on the levelised cost of wind energy', *Renewable Energy*, 101. Available at: https://doi.org/10.1016/j.renene.2016.09.003.

Heidarzadeh, M. *et al.* (2023) 'Normal and reverse storm surges along the coast of Florida during the September 2022 Hurricane Ian: Observations, analysis, and modelling', *Ocean Modelling*, 185, p. 102250. Available at: https://doi.org/10.1016/j.ocemod.2023.102250.

Hendy, D.M. *et al.* (2021) 'Sea level characteristics and extremes along Alexandria coastal zone', *Arabian Journal of Geosciences*, 14(13). Available at: https://doi.org/10.1007/s12517-021-06863-4.

Ibrahim, O. and El-Gindy, A. (2022) 'Comprehensive analysis of monthly mean sea level in the Eastern Mediterranean as a tool for prediction and risk assessment of future expected sea level rise', *Arabian Journal of Geosciences*, 15(1), p. 3. Available at: https://doi.org/10.1007/s12517-021-08845-y.

Jansen and Paasche, Ø. (2007) *IPCC [Intergovernmental Panel on Climate Change]. Climate Change 2007: The Physical Science Basis. Contribution of Working Group I to the Fourth Assessment Report of the IPCC. Cambridge, United Kingdom Cambridge University Press*.

Lira-Loarca, A. *et al.* (2021) 'Future wind and wave energy resources and exploitability in the Mediterranean Sea by 2100', *Applied Energy*, 302, p. 117492. Available at: https://doi.org/10.1016/j.apenergy.2021.117492.

Maiyza, I.A. and El-Geziry, T.M. (2012) 'Long term sea-level variation in the south-eastern Mediterranean Sea: A new approach of examination', *Journal of Operational Oceanography*, 5(2). Available at: https://doi.org/10.1080/1755876X.2012.11020138.

McInnes, K. *et al.* (2015) 'Information for Australian impact and adaptation planning in response to sea-level rise', *Australian Meteorological and Oceanographic Journal*, 65(1), pp. 127–149. Available at: https://doi.org/10.22499/2.6501.009.

Medvedev, I.P., Rabinovich, A.B. and Kulikov, E.A. (2016) 'Tides in Three Enclosed Basins: The Baltic, Black, and Caspian Seas', *Frontiers in Marine Science*, 3. Available at: https://doi.org/10.3389/fmars.2016.00046.

Nabil N. Saad (2011) 'Water heights and weather regimes at Alexandria Harbor', *International Journal of the Physical Sciences*, 6(30). Available at: https://doi.org/10.5897/IJPS11.018.

Noby, M., Michitaka, U. and Hamdy, O. (2022) 'Urban Risk Assessments: Framework for Identifying Land-uses Exposure of Coastal Cities to Sea Level Rise, a Case Study of Alexandria', *SVU-International Journal of Engineering Sciences and Applications*, 3(1), pp. 78–90. Available at: https://doi.org/10.21608/svusrc.2022.132215.1045.

on Climate Change IPCC, I.P. (2013) 'AR5 Climate Change 2013: The Physical Science Basis — IPCC'. IPCC. Available at: https://www.ipcc.ch/report/ar5/wg1/.

Ozturk, M. and Yuksel, Y. (2023) 'Tidal and non-tidal sea level analysis in enclosed and inland basins: The Black, Aegean, Marmara, and Eastern Mediterranean (Levantine) Seas', *Regional Studies in Marine Science*, 61, p. 102848. Available at: https://doi.org/10.1016/j.rsma.2023.102848.

Parker, B. (2007) 'Tidal Analysis and Prediction Center for Operational Oceanographic Products and Services. '. Available at: https://tidesandcurrents.noaa.gov/.

Pawlowicz, R., Beardsley, B. and Lentz, S. (2002) 'Classical tidal harmonic analysis including error estimates in MATLAB using T_TIDE', *Computers & Geosciences*, 28(8), pp. 929–937. Available at: https://doi.org/10.1016/S0098-3004(02)00013-4.

Pugh, D. (1987) *Tides, Surges and Mean Sea Level: A Handbook for Engineers and Scientists.* John Wiley & Sons, Chichester.

Pugh, D. and Woodworth, P. (2014) *Sea-Level Science*, *Sea-Level Science*. Available at: https://doi.org/10.1017/cbo9781139235778.

Pugh, D.T. (2004) *Changing sea levels: Effects of tides, weather, and climate*. Cambridge University Press.

Radwan, A.A. and El-Geziry, T.M. (2013) 'Some statistical characteristics of surges at alexandria, egypt', *Journal of King Abdulaziz University, Marine Science*, 24(2). Available at: https://doi.org/10.4197/Mar.24-2.3.

Rignot, E. *et al.* (2011) 'Acceleration of the contribution of the Greenland and Antarctic ice sheets to sea level rise', *Geophysical Research Letters*, 38(5), p. n/a-n/a. Available at: https://doi.org/10.1029/2011GL046583.

Said, M., Moursy, Z.A. and Radwan, A.A. (2012) 'Climate change and sea level oscillations off Alexandria, Egypt', *International Conference Mar Coast Ecos* [Preprint].

Shaker, A. *et al.* (2011) 'Absolute Sea Level Rise Estimation at Alexandria Using Tide Records and GPS Observations', in *FIG WORKING WEEK,BRIDGING THE GAP BETWEEN CULTURES*.

Shaltout, M. and Omstedt, A. (2014) 'Recent dynamic topography changes in the Mediterranean Sea analysed from Satellite altimetry data', *Curr Dev Oceanogr* [Preprint].

MRT
ISSN 2812-5622
http://dx.doi.org/10.21622/MRT.2025.04.1.1110

Shepherd, A. *et al.* (2012) 'A reconciled estimate of ice-sheet mass balance', *Science*, 338(6111). Available at: https://doi.org/10.1126/science.1228102.

Tsimplis, M. *et al.* (2009) 'Sea level variability in the Mediterranean Sea during the 1990s on the basis of two 2d and one 3d model', *Journal of Marine Systems*, 78(1). Available at: https://doi.org/10.1016/j.jmarsys.2009.04.003.

Wada, Y. *et al.* (2012) 'Past and future contribution of global groundwater depletion to sea-level rise', *Geophysical Research Letters*, 39(9). Available at: https://doi.org/10.1029/2012GL051230.

Weisberg, R.H. and Zheng, L. (2006) 'Hurricane storm surge simulations for Tampa Bay', *Estuaries and Coasts*, 29(6). Available at: https://doi.org/10.1007/BF02798649.

Zerbini, S. and Vincent, R.F. (2014) 'Sea level trends in the Mediterranean from tide gauges and satellite altimetry'.